Progress In Electromagnetics Research Letters, Vol. 84, 115–121, 2019

Miniaturized HMSIW Bandpass Filter Based on the Coupling of Dual-Iris with Nested Stepped-Impedance CSRRs

Bo Yin, Zhangyao Lin*, Honggang Hao, Wei Luo, and Wen Huang

Abstract—A novel miniaturized bandpass half-mode substrate integrated waveguide (HMSIW) filter which uses dual-iris coupling method to load complementary split-ring resonators (CSRRs) into HMSIW is proposed in this paper. By modifying traditional CSRRs through nesting method combined with step impedance structure, a nested stepped-impedance complementary split-ring resonator (NSICSRR) structure with higher equivalent capacitance and inductance of CSRR is obtained. Based on the traditional single-iris coupling method, a dual-iris coupling method is developed. And NSICSRR is loaded into HMSIW by using the dual-iris coupling method, which can reduce the resonant frequency of the structure. In order to verify the effectiveness of the technology above in realizing the miniaturization of HMSIW filter, a second-order HMSIW filter is designed and measured. It can be found in the measured results that the filter has the center frequency of 6.35 GHz, the 3 dB bandwidth of 690 MHz, the return loss of better than 14 dB within the passband, and the size of $0.0396\lambda_g^2$. The experimental results are basically consistent with the simulation ones.

1. INTRODUCTION

Since Deslandes and Wu proposed the substrate integrated waveguide (SIW) structure and designed a Ka-band Chebyshev filter based on it in 2003, SIW has been considered as a potential alternative structure for the integration of wireless communication, radar, and sensing systems [1]. SIW not only has the characteristics of low loss, low radiation, high Q value, and high power capacity of rectangular metal waveguide, but also has advantages of small size and easy integration. So it is widely used in antenna, filter, and other RF devices. Nowadays, the research of SIW is developing towards higher performance and miniaturization. The appearance of HMSIW and quadruple-mode substrate integrated waveguide (QMSIW) makes it possible to maintain a similar performance with only half or a quarter of the SIW size [2, 3].

As a metamaterial structure, the CSRR provides a new resonant frequency for SIW filter by using electric field of microstrip and does not increase the circuit size, which greatly promotes the miniaturization of SIW filter [4]. Huang et al. developed a horizontal asymmetric SICSRR and loaded it into HMSIW to form a resonant unit, which can have lower frequencies than traditional HMSIW-CSRR resonators when occupying the same physical circuit size [5]. Xu et al. and Huang et al. combined defected ground structure (DGS) technology with half-mode substrate integrated waveguide (HMSIW) to design a miniaturized dual-pass filter by loading CSRRs with double-sided loading technology [6, 7]. Danaeian et al. used a stepped-impedance resonator (SIR) to reduce the physical size of traditional CSRR, designing a compact metamaterial element SIR-CSRR and loaded it into HMSIW [8].

In this paper, nested stepped-impedance complementary split-ring resonators (NSICSRRs) are developed and loaded into HMSIW to form a resonant unit. Compared with the traditional resonant

Received 26 February 2019, Accepted 12 May 2019, Scheduled 31 May 2019
* Corresponding author: Zhangyao Lin (s170401001@stu.cqupt.edu.cn).
The authors are with the College of Optoelectronic Engineering, Chongqing University of Posts and Telecommunications, Chongqing, China.

element, the designed resonant element with the same size can work at a lower resonant frequency. Then, based on the traditional single iris coupling method, a dual-iris coupling method is proposed, which is used in the design of a band-pass filter. Compared with a single iris coupled bandpass filter and direct coupled band-pass filter, the space between NSICSRR resonant units in a dual-iris coupled band-pass filter is the smallest. Finally, the nested step impedance technology is loaded into HMSIW by dual-iris coupling method, and a miniaturized bandpass filter is designed, which is simulated, analyzed, and measured.

2. THE DESIGN OF BANDPASS FILTER

2.1. HMSIW-NSICSRR Resonator

Figure 1 shows the evolution of an NSICSRR structure, which is as follows: it nests two kinds of single-loop CSRRs with a step impedance (SI) structure. For a traditional CSRR and proposed NSICSRR, their equivalent circuit models can be simplified to inductance and capacitance (LC) circuits in parallel, as shown in Fig. 2. Therefore, their operating frequency can be expressed as:

$$f_c = \frac{1}{2\pi\sqrt{L_0 C_0}} \quad (1)$$

$$f_{c\text{NSI}} = \frac{1}{2\pi\sqrt{L_{\text{NSI}} C_{\text{NSI}}}} \quad (2)$$

where L_0 and L_{NSI} represent the equivalent inductance of CSRR and NSICSRR, respectively. C_0 and C_{NSI} represent the equivalent capacitance of CSRR and NSICSRR, respectively.

Obviously, by adjusting the impedance ratio and phase ratio of NSICSRR, slow wave effect can be effectively generated, and the resonant frequency of NSICSRR can be reduced.

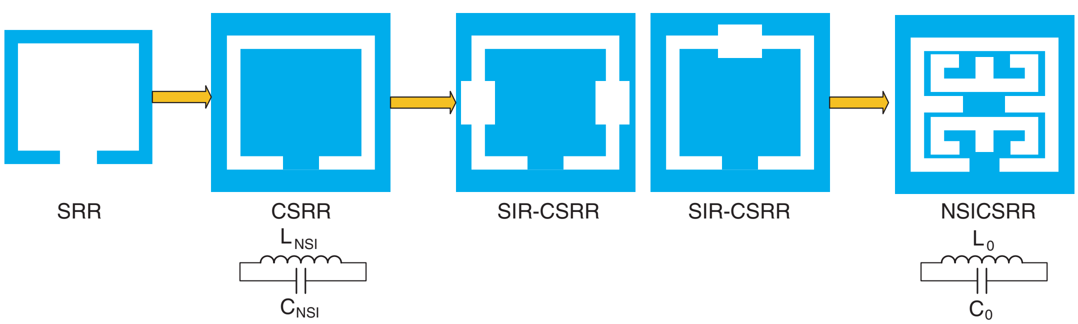

Figure 1. The evolution of the proposed NSICSRRs structure.

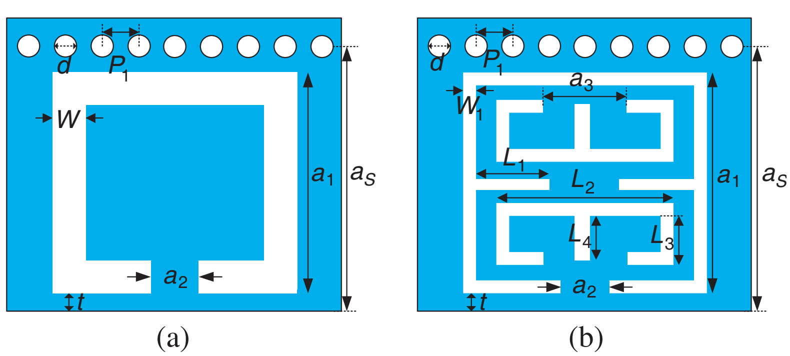

Figure 2. (a) Traditional HMSIW-CSRR resonant unit, (b) proposed HMSIW-NSICSRR resonant unit.

The HMSIW-NSICSRR resonant unit is obtained through loading NSICSRR in the surface of HMSIW as shown in Fig. 2(b), while the traditional HMSIW-CSRR resonant unit is as shown in Fig. 2(a). To describe the transmission characteristics of the proposed NSICSRR resonant unit more clearly, the analyses are processed with a commercial FEM simulator, and an RT/duroid 5880 dielectric substrate with thickness of 0.508 mm is selected, with relative dielectric constant of 2.2 and loss tangent of 0.001. As can be easily seen from Fig. 3, the HMSIW structure loaded with CSRR can produce a transmission pole lower than the cutoff frequency of the traditional HMSIW. Moreover, the HMSIW structure loaded with NSICSRR produces the pole at the frequency of 6.01 GHz when w is 0.2 mm, while the HMSIW structure loaded with traditional CSRR produces the pole at 6.37 GHz and 6.66 GHz when w is 0.2 mm and 0.4 mm, respectively. Since the size of the physical circuit of cell is determined by w and b, the proposed HMSIW-NSICSRR resonant unit has a higher equivalent tolerance than the HMSIW-CSRR resonant unit, which enables it to get a lower resonant frequency at the same physical size. At the same time, the proposed HMSIW-NSICSRR resonant unit has higher frequency selectivity, because its transmission zero is nearer to center frequency than that of HMSIW-CSRR resonant unit.

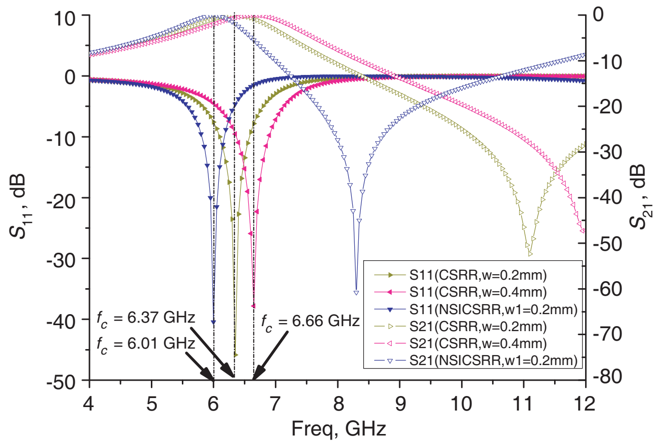

Figure 3. Simulated results comparison between traditional HMSIW-CSRR unit and proposed HMSIW-SICSRR unit.

2.2. The Design of Second Order Bandpass Filter

Based on the HMSIW-NSICSRR resonant unit proposed above, the design idea of the second-order bandpass filter in this paper is shown by deducing from Fig. 4(a) to Fig. 4(c), where Fig. 4(a) shows the direct coupling scheme without iris loading; Fig. 4(b) shows the coupling scheme with single iris loading; and Fig. 4(c) shows the coupling scheme with dual-iris loading.

In this paper, the classical filter design method is used to determine the relative bandwidth, in which the main design parameters are the coupling coefficient (M_{12}) between resonant units. The resonant mode of the second order resonator is divided into two modes, namely the even mode and odd mode (taking the dual-iris as an example in Fig. 5), in which the electric field of the even mode has symmetrical distribution, and the electric field of the odd mode has anti-symmetrical distribution. According to the resonant frequencies of the two modes, the relationship between the coupling coefficient (M_{12}) and coupling spacing of the three kinds of coupling scheme can be extracted by Equation (3), and the result is shown in Fig. 6.

$$M_{12} = \frac{\left(f_{\text{odd}}^2 - f_{\text{even}}^2\right)}{\left(f_{\text{odd}}^2 + f_{\text{even}}^2\right)} \quad (3)$$

In Fig. 6, it can be seen that the loaded iris structure can obtain the same coupling coefficient (M_{12}) with smaller coupling spacing, so as to realize miniaturization. Under the condition of smaller coupling spacing, the dual-iris structure can obtain the same coupling coefficient (M_{12}) loaded with smaller coupling spacing than the single iris structure, which further realizes miniaturization.

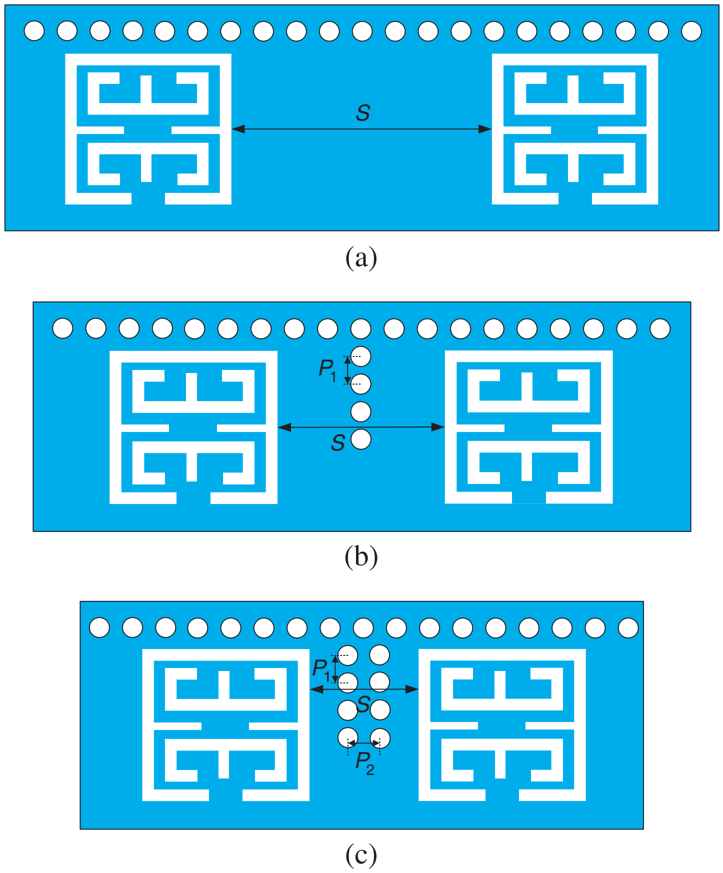

Figure 4. (a) Direct coupling scheme, (b) coupling scheme with single iris loading, (c) coupling scheme with dual-iris loading.

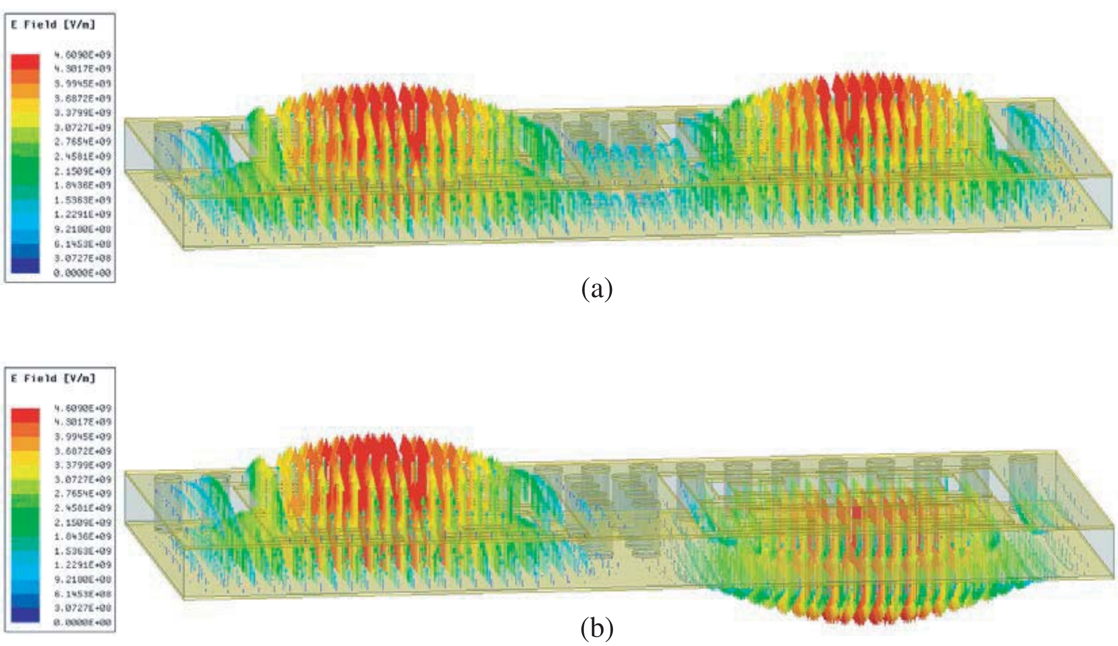

Figure 5. The resonant mode of the second order resonator with the dual-iris loading, (a) even mode, (b) the odd mode.

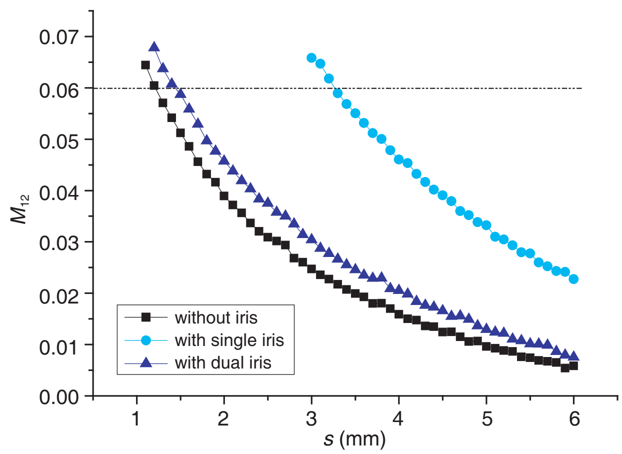

Figure 6. Simulated results comparison between coupling scheme with direct loading, single iris loading and dual-iris loading.

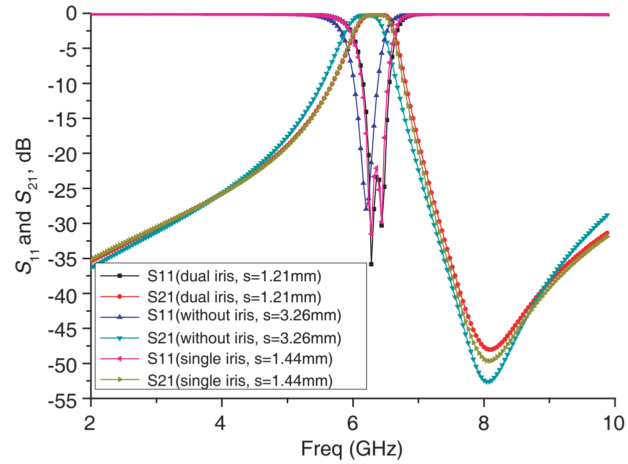

Figure 7. Simulated results of the HMSIW-NSICSRR bandpass filter with different kind of coupling schemes.

Three kinds of coupling schemes are applied into filters, whose metal layer is copper with a thickness of 30 μm. In this paper, coupling spacing of filters is determined by selecting the same coupling coefficient $M_{12} = 0.06$. The purpose of the same coupling coefficient is to verify that the coupling scheme of dual iris can reduce the size of the filter without adverse effects compared with the other two. Fig. 6 shows that when $M_{12} = 0.06$, the coupling spacing of the filter without iris is 3.26 mm; the coupling spacing of the filter with single iris is $s = 1.44$ mm; and the coupling spacing of the filter with dual iris is 1.21 mm. The simulation results through commercial FEM simulator are shown in Fig. 7. Some of optimized parameters are mentioned in Table 1.

Table 1. Design parameter value.

Parameter	unit (mm)	Parameter	unit (mm)	Parameter	unit (mm)
d	0.30	p_1	0.50	a_s	4.10
a_1	3.50	a_2	0.40	t	0.20
w_1	0.20	L_1	0.85	L_2	2.60
L_3	0.80	L_4	0.70	a_3	1.00
p_1	0.52	p_2	0.50		

As can be seen from Fig. 7, when the coupling coefficients are the same, the filters based on the three coupling schemes show similar performances. The filter without iris has central frequency of 6.25 GHz and 3 dB bandwidth of 680 MHz; the filter with single iris has central frequency of 6.36 GHz and 3 dB bandwidth of 670 MHz; and the filter with dual iris has central frequency of 6.36 GHz and 3 dB bandwidth of 680 MHz. Although loading iris structure produces some frequency shift, it is acceptable compared with size reduction. The filter with dual iris has almost the same performance as the filter with single iris. In summary, the coupling scheme of dual iris can reduce the size of the filter, while it meets similar performance specifications. The design of filter using dual iris coupling scheme in this paper, is shown in Fig. 8.

3. RESULTS AND DISCUSSIONS

To demonstrate the design, the proposed filter is fabricated and measured, which is presented in Fig. 9. The processed sample is examined by an SMA connector and Agilent N5242A PNA-X Vector network

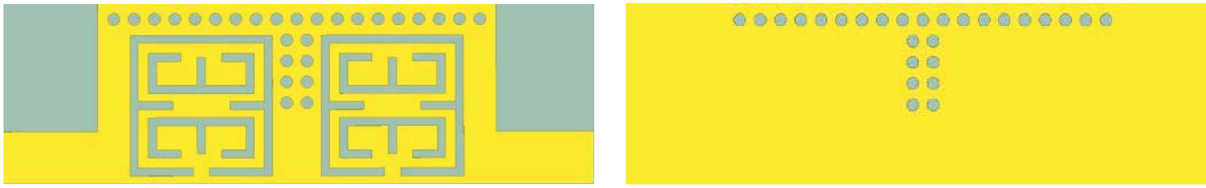

(a) (b)

Figure 8. Structure diagram of the HMSIW-NSICSRR bandpass filter, (a) top view, (b) bottom view.

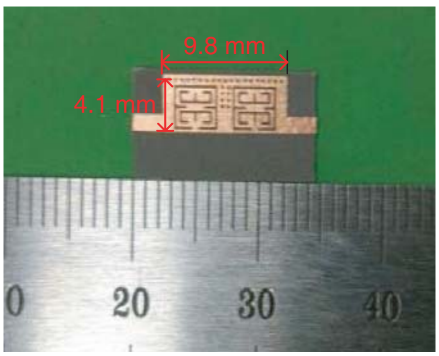

Figure 9. Photograph of the HMSIW-NSICSRR filter.

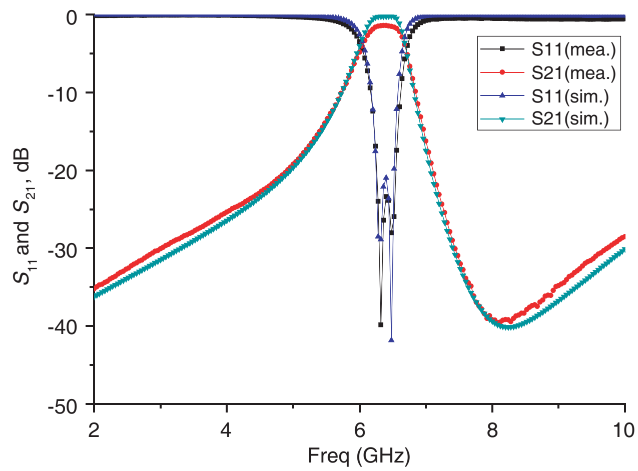

Figure 10. Simulated and measured S-parameters for HMSIW-NSICSRR filter.

analyzer. The measurement results are shown in Fig. 10.

Figure 9 shows the HMSIW-NSICSRR filter with a compact size of 9.8 mm × 4.1 mm (i.e., $0.0396\lambda_g^2$, λ_g is the guided wavelength at 6.35 GHz). As shown in Fig. 10, the center of the measured passband is about 6.35 GHz, and the 3 dB bandwidth is about 690 MHz, which is almost the same as that of simulation. The simulated insertion loss at 6.36 GHz is about 0.24 dB, and the measured insertion loss at 6.35 GHz is about 1.06 dB. The return loss is better than 14 dB within the passband. Some discrepancies in frequency shift, In-band flatness levels, and insertion loss levels are observed. First, the tolerances of the dielectric constant, 2.20 ± 0.02, may result in a small frequency shift and affect attenuation levels. Second, soldering (manual) of coax connectors to the microstrip ports of the filter circuit may affect in-band flatness levels and insertion loss levels. Third, machining tolerance may result in a small frequency shift, in-band flatness levels, and insertion loss levels. The comparison between the proposed structure and some other miniaturized bandpass filters is presented in Table 2.

Table 2. Comparison between the proposed and referenced filters.

Ref.	Order	Substrate Thickness (mm)	f_0 (GHz)	FBW (%)	Insertion Loss (dB, @ f_0)	Return Loss [dB]	Size [λ_g^2]
[5]	2	0.508	8.40	7.90	1.53	> 10	0.042
[9]	2	0.787	2.45	8.20	0.90	> 10	0.051
[10]	3	0.254	10.00	23.00	1.20	> 10	0.257
This Work	2	0.508	6.35	10.86	1.06	> 14	0.039

4. CONCLUSIONS

In this paper, an improved HMSIW-CSRR bandpass filter with coupling scheme of dual-iris and loaded with the proposed NSICSRRs has been designed, fabricated, and measured. Loading NSICSRRs structure can get lower resonance frequency without increasing physical size. By using dual-iris coupling, the same coupling coefficient can be obtained with smaller coupling spacing. Therefore, based on the coupling of dual-iris, proposed NSICSRRs etched on the top surfaces of the HMSIW cavity, the proposed filter has a compact size, as well as good insertion loss. It is worth noting that the filter does not exhibit excellent outstanding out-of-band performance and rectangular coefficient, but geometry of the proposed filter allows the loading of DGS structure while keeping small size to improve out-of-band rejection and the rectangular coefficient.

ACKNOWLEDGMENT

This work is supported by the National Natural Science Foundation of China (Grant Nos. 41606203 and 61601074), the Chongqing Education Commission's Science (Grant Nos. KJ1600438, KJ1600409 and KJ1600421) and Technology Research Project and the Chongqing basic Science and Frontier Technology Research Project (Grant Nos. cstc2017jcyjAX0193, cstc2018jcyjAX0508 and cstc2017jcyjAX0128).

REFERENCES

1. Deslandes, D. and K. Wu, "Single-substrate integration technique of planar circuits and waveguide filters," *IEEE Transactions on Microwave Theory and Techniques*, Vol. 51, No. 2, 593–596, 2003.
2. Liu, B., W. Hong, Y. Zhang, J. X. Chen, and K. Wu, "Half-mode substrate integrated waveguide (HMSIW) double-slot coupler," *Electronics Letters*, Vol. 43, No. 2, 113–114, 2007.
3. Huang, Y. M., Z. Shao, C. J. You, and G. Wang, "Size-reduced bandpass filters using quarter-mode substrate integrated waveguide loaded with different defected ground structure patterns," *IEEE MTT-S International Microwave Symposium*, 1–4, Phoenix, USA, 2015.
4. Choudhury, A. and S. Maity, "Design and fabrication of CSRR based tunable mechanically and electrically efficient band pass filter for K-band application," *International Journal of Electronics and Communications*, Vol. 72, 134–148, 2017.
5. Huang, Y. M., Z. Shao, W. Jiang, T. Huang, and G. Wang, "Half-mode substrate integrated waveguide bandpass filter loaded with horizontal-asymmetrical stepped-impedance complementary split-ring resonators," *Electronics Letters*, Vol. 52, No. 12, 1034–1036, 2016.
6. Huang, Y. M., Y. Peng, Y. Zhou, H. Jin, S. Leng, and G. Wang, "Size-reduced dual-band HMSIW cavity filters loaded with double-sided SICSRRs," *Electronics Letters*, Vol. 53, No. 10, 689–691, 2017.
7. Xu, S., K. Ma, F. Meng, and K. S. Yeo, "Novel defected ground structure and two-side loading scheme for miniaturized dual-band SIW bandpass filter designs," *IEEE Microwave and Wireless Components Letters*, Vol. 25, No. 4, 217–219, 2015.
8. Danaeian, M., K. Afrooz, and A. Hakimi, "Miniaturization of substrate integrated waveguide filters using novel compact metamaterial unit-cells based on SIR technique," *International Journal of Electronics and Communications*, Vol. 84, 62–73, 2018.
9. Azad, A. R. and A. Mohan, "Sixteenth-mode substrate integrated waveguide bandpass filter loaded with complementary split-ring resonator," *Electronics Letters*, Vol. 53, No. 8, 546–547, 2017.
10. Wang, C., Z. Wang, and Y. M. Huang, "Size-miniaturized half-mode substrate integrated waveguide bandpass filter incorporating E-shaped defected ground structure for wideband communication and radar applications," *20th International Conference on Advanced Communication Technology (ICACT) Technol.*, 12–16, Chuncheon-si, Korea (South), 2018.